A port-Hamiltonian framework for operator force assisting systems: application to the design of helicopter flight controls

Matthieu Touron[a], Jean-Yves Dieulot[b], Julien Gomand[a], Pierre-Jean Barre[a]

[a] *Arts et Metiers ParisTech, CNRS LSIS, 13100 Aix-en-Provence, France*
[b] *CRIStAL UMR CNRS 9189, Polytech-Lille/MOCIS Cité Scientifique 59650 Villeneuve d'Ascq France (Email: dieulot@univ-lille1.fr)*

Abstract

An energetic representation of helicopter flight controls, viewed as an Operator Assisting System, is proposed within the Port-Hamiltonian framework. The assisting controller modifies the dynamical behavior between the pilot stick and the swashplate, linked through a Continuous Variable Transmission, by enforcing force scaling and providing appropriate force feedback to the operator. Generic sufficient conditions are given on the assistance location and structure which allow the assisted system to be dissipative, hence providing nice stability and power scaling properties. Results are applied to the design of an assistance for a simplified flight control system. Simulations show the relevance of the method and are compared to real-life results.

Keywords: Port-Hamiltonian, Helicopter, Flight-Axis control, Assisting system, passivity

1. INTRODUCTION

Helicopter flight controls help the pilot to modify the motion of the rotor blades which will in turn move the aircraft. The cyclic control changes the pitch of the blades cyclically, steering the angle of attack and the lift generated by each blade, tilting the rotor into a particular direction. A swashplate allows to turn the displacements resulting from the flight controls into a rotating motion

of the blades, which will be detailed further (Raletz (2010), Torenbeek and Wittenberg (2009)). The main goal of flight controls is to give an assistance to the pilot, which moves a stick, by providing extra power to actuate the swashplate (McKillip and Perri (1992), Lee et al. (2005), Simplício et al. (2013)). In almost all current helicopters, this is achieved through a mechanical Continuous Variable Transmission (CVT) and hydraulic assisting devices, and there is no fly-by-wire, that is no teleoperation. Real helicopter flight controls are far more complicated than power scaling devices, because additional sub-elements allow to achieve different specifications (e.g. trim control, vibration control, automatic pilot control...); however, these elements often interact and their tuning is not simple (Friedman and Rand (2015)).

Nevertheless, the main question which is addressed in this paper remains to design a power assistance which will be able to actuate the swashplate and generate an appropriate force feedback for the pilot. While the classical approach focuses on shaping the impedance, either of the operator or the load (Hogan (1985); Lacevic and Rocco (2011); Worsnopp et al. (2006)), it seems consistent to study the power flows within the CVT (Kazerooni (1990)), using energetic representations of multiphysics systems such as Bond Graphs (Richter (2015); Li and Ngwompo (2005)). These systems interact with external force or flow sources through terminals called ports. Li and Ngwompo (2005) showed that power amplification could result from a scaling between the forces (resp. flow) of the operator and environment, which they called Power Transformer (PTF), or a scaling between the flow of one port and the force of another, named Power Gyrator (PGY). As a companion model, a Port-Hamiltonian system is a passive power-based state-space representation that can be derived from a Bond-Graph (Donaire and Perez (2012)). Passivity is an important property, as passive Port-Hamiltonian systems enjoy equilibrium stability and asymptotic stabilization by negative output feedback. Further, control laws can be generically derived from this representation by assigning the desired total or potential energies of

the closed-loop system (Donaire and Perez (2012); Crasta et al. (2015); Ortega et al. (2002); Zhu et al. (2012)), e.g. changing this energy to shift the equilibrium to a new one.

The pilot assistance scheme belongs to a class of Operator Assisting Systems (OAS) which consists of devices that help a human user to control and interact with his environment (a "load") through a CVT (Kazerooni (1990)). The assistance allows the operator to scale his power up, therefore modifying the dynamics between the operator a)nd its environment. These systems find applications in various domains, such as power steering, electric tools, medicine (assisted surgery, protheses), etc. (De Santis et al. (2008); Worsnopp et al. (2006)).
In this paper, it will be shown that such an Operator Assisting System (OAS) can be considered as a unique Port-Hamiltonian system (the CVT) with several ports, including an operator port (the pilot), a load port (the swashplate) and external ports through which an assistance can be applied (Kazerooni (1990)). The main contribution will be to find the application points and structure of this assistance so that the scaled system (operator-swashplate) is passive. Hence, through this framework, the assistance control design can be handled in a systematic and generic fashion.

Teleoperation shares the notion of "assistance" with OAS, but its frame is fairly different. Teleoperation is a remote control of the flow and effort from one subsystem (the slave) with respect to the behavior of another system (the master), linked through communication buses (e.g. Secchi et al. (2007); Ferraguti et al. (2015); Wang and Xie (2012); Jazayeri and Tavakoli (2016)). However, for OAS, the assistance can be considered as one out of the three ports of a unique physical system (the CVT), that modifies the relation between the flows and efforts from the two other external ports, that is the operator and the load. Classical closed-loop control aims at steering an output towards a reference trajectory, and generates an autonomous system. This is not the case for assistive

control, which goal consists of enforcing new dynamics between uncontrolled inputs and outputs (forces and flows attached to the operator and environment). This paper shows also how to adapt energetic methods to the specific case of Operator Assisting Systems. Hence, it will be shown that the 3 (or more)-port system has to be transformed into a closed-loop two-port system.

First, current flight controls will be described and the main assistance specifications will be discussed. Then, it will be shown that the flight controls can be represented by a Port-Hamiltonian system with at least three ports. The paper will then explore the conditions under which the assistance generates a dissipative force-scaling system. The results will be applied to the specific case of helicopter flight controls; simulations of the simplified system under assistance will be compared to a simulated multibody model, close to the actual system, and to experimental results, showing the relevance of the control design.

2. Energetic Representations and dissipative-based control of Operator Assisting Systems

2.1. Three-port linear representation and control objectives

In this paper, only the restricted class of OAS following Definition 1 will be considered:

Definition 1. *An Operator Assisting System is a physical CVT manipulator with an assistance that enforces specified dynamical interactions between a unique operator and a unique load (environment).*

The definition assumes that only physically continuous systems will be considered for which the assistance is located at least at one port (interface where power is exchanged). From the mathematical point of view, when the dynamics is linear and there is just one point of application of the assistance, the Operator Assisting System can be considered as a three-port model, which is an extension of the two-port model often used for teleoperation (see Secchi et al. (2007) for a

review). This representation allows to characterize the energetic interaction between the operator, load and assistance in terms of inputs and outputs, namely efforts and velocities, measurable at three sets of terminals or ports. Of these six variables, three can be found as "dependent" (outputs), and the remaining ones as "independent" (inputs), which results from the causal analysis of the system (cf. Figure 1). For the case where the load effort and operator velocities are the independent variables, one obtains:

$$\begin{bmatrix} f(s) \\ v(s) \\ b(s) \end{bmatrix} = \begin{pmatrix} h_{11}(s) & h_{12}(s) & h_{13}(s) \\ h_{21}(s) & h_{22}(s) & h_{23}(s) \\ h_{31}(s) & h_{32}(s) & h_{33}(s) \end{pmatrix} \begin{bmatrix} u(s) \\ e(s) \\ a(s) \end{bmatrix} \tag{1}$$

where u, f, v, e are respectively the operator velocity and effort, load velocity and effort, a is the velocity/effort of the assistance and b is the dual variable (velocity or effort), s is the Laplace variable. a represents the assistance actuation, and b the reaction of the system on the actuator; product $a.b$ is related to assiting power and is a good indicator for actuator design. Without assistance, the input-output behavior reduces to the well-known hybrid-parameter matrix (or H-matrix, see (Secchi et al. (2007))). There are other configurations depending whether the inputs and outputs are flows and/or efforts. For example, if the inputs are the velocities, and outputs are forces, the matrix giving the relations between inputs and outputs will be called an impedance matrix (e.g. see Secchi et al. (2007)). While the H-matrix is a standard representation in teleoperation systems, these consider a master robot directly driven by the operator, and a slave robot located in remote environment, which will follow any trajectory ordered by the master through a virtual interface. In the OAS case, the assistance can be considered as an external source acting directly on the manipulator, and thus adds an extra port to this system.

The aim of the assistance is to modify the system of equation (1) to meet the desired closed loop behavior represented by the two-port matrix $\mathbf{H_d}(\mathbf{s}) = (h_d\{ij\}(s))$ in equation (2). The expression of b is not given, as the goal of the assistance is not to shape the relation a, b.

$$\begin{bmatrix} f(s) \\ v(s) \end{bmatrix} = \begin{pmatrix} h_{11_d}(s) & \gamma_E h_{12_d}(s) \\ \gamma_F h_{21_d}(s) & h_{22_d}(s) \end{pmatrix} \begin{bmatrix} u(s) \\ e(s) \end{bmatrix} \tag{2}$$

γ_F, γ_E are flow and effort scaling factors. Matrix $\mathbf{H_d}$ can be interpreted easily physically, as h_{11_d} is the specified unconstrained movement normalized impedance, h_{21_d} is the transfer function of scaled velocity tracking, h_{12_d} is related to force scaling, and h_{22_d} can be called normalized contact admittance (Ferraguti et al. (2015)). In our case example, the inputs are the swashplate torque and the pilot stick velocity, the outputs are the stick feedback effort and the swashplate pitch velocity. Extra power is needed to move the swashplate and force feedback should be brought to the pilot.

It is possible, for the closed-loop assisted system, to use the terminology of teleoperated systems to characterize the dynamics. Considering the case in the present paper, for which inputs are slave effort and master flow, Hannaford (1989) has shown that, for perfect scaling, the H-matrix should be (see e.g. Secchi et al. (2007)) :

$$\mathbf{H_d} = \begin{pmatrix} 0 & \gamma_E \\ \gamma_F & 0 \end{pmatrix} \tag{3}$$

where $\gamma_F = 1$ for force scaling. When $\gamma_F = \gamma_E = 1$, the slave system reproduces the behavior of the master system with fidelity, the impedance from the master and the slave side are equal, and the system is called transparent (Secchi et al. (2015)). For OAS, this will never be possible to achieve perfect transparency because of the closed-loop dynamics, which depends both on the assistance control and the CVT dynamics. While designing a closed-loop assisted system (3) from representation (1) seems easy, the latter however has some drawbacks as it shows only the input/ouptut relations and not the power flows and energy storages within the system, and is also not appropriate for nonlinear systems.

2.2. Port-Hamiltonian systems and Operator Assisting Systems

As the system is physically continuous and involves power flows, it is possible to use the Bond-Graph formalism. A Bond-Graph is a graphical description

which unveils the management of energy in a physical system (storage represented by C- or I- , i.e. capacitive or inertial elements, dissipation represented by R-, i.e. resistor elements, etc.), as will be illustrated by the example. It exhibits the interconnection structure through which internal and external (flow and effort sources) power exchange occurs, allowing to find causal relationships between physical variables. Bond-Graphs are best suited to analyze the structural controllability of a system, and used for fault detection, sensor/actuator design, etc., but are less devoted to control design. However, power scaling cannot be represented by a real Bond-Graph element (as there is no power conservation) but by a so-called Power Transformer (PTF) which modulates the power through an external parameter (Li and Ngwompo (2005)) as follows:

$$PTF : f_1 = m_F f_2; e_1 = m_E e_2 \tag{4}$$

where f_1, f_2, e_1, e_2 are respectively flows and efforts at ports 1 and 2, m_F, m_E are scalars. A companion state-space representation of Bond-Graphs is the so-called Port-Hamiltonian form, which synoptic is shown in Figure 1.

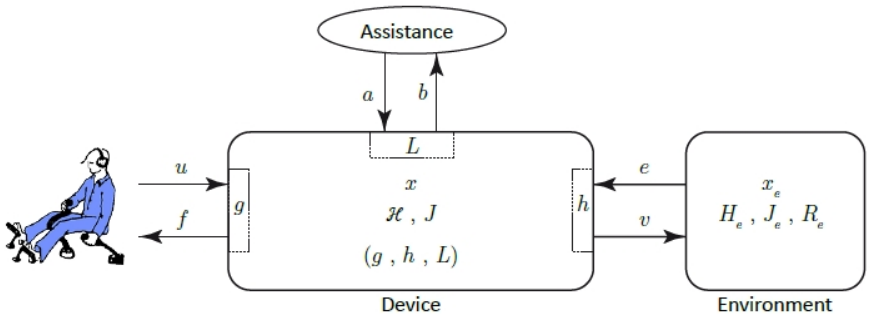

Figure 1: A representation of Port-Hamiltonian systems under assistance and environment

Consider the total energy $\mathcal{H}(\mathbf{x})$ of a CVT subjected to external sources, where $\mathbf{x}$ is the energetic state vector. The operator velocity u, the load (environment) effort e, and their collocated responses f and v are scalars, whereas

the assistance is represented by the vector $\mathbf{a}$. f,u (resp. e,v) are called the operator (resp. load) port power variables, their duality product defines the power flows exchanged at the operator (resp. load) port. The system in Figure 1 can be put under the Port-Hamiltonian form of equation (5), which embeds the total (kinetic and potential) energy and is valid for linear and nonlinear systems. Donaire and Perez (2012):

$$\begin{cases} \dot{\mathbf{x}} = (\mathbf{J}(\mathbf{x}) - \mathbf{R}(\mathbf{x}))\frac{\partial \mathcal{H}}{\partial \mathbf{x}} + \mathbf{g}.u + \mathbf{h}.e + \mathbf{L}.\mathbf{a} \\ f = \mathbf{g}^T \frac{\partial \mathcal{H}}{\partial \mathbf{x}}, v = \mathbf{h}^T \frac{\partial \mathcal{H}}{\partial \mathbf{x}}, b = \mathbf{L}^T \frac{\partial \mathcal{H}}{\partial \mathbf{x}} \end{cases} \tag{5}$$

where $\mathbf{J}(\mathbf{x})$ is the skew-symmetric interconnection matrix, $\mathbf{R}(\mathbf{x})$ is the symmetric dissipation matrix, $\mathbf{g},\mathbf{h}$ are input vectors. The main goal of the control design will be to determine the global assistance $\mathbf{L}.\mathbf{a}$. $\mathbf{L}$ is the assistance input matrix that can be seen as indicating the location of the assistance within the CVT and $\mathbf{a}$ is the control vector corresponding to the structure of this assistance. Assistance is assumed to be located at an external port of the CVT. Hence, the maximum number of application points cannot exceed the dimension of the system n, matrix $\mathbf{L}$ has dimensions $n \times n$, and product $\mathbf{L}.\mathbf{a}$ has the dimension of the state space vector $\mathbf{x}$ (of course, some of its elements can be zero).

2.3. Dissipativity-Based-Control of Operator Assisting Systems

A passive system is a system which cannot store more energy than is supplied by some source, with the difference between the stored energy and supplied energy, being the dissipated energy.

Definition 2. *(see e.g. Bao and Lee (2007)) Let the nonlinear system noted (NLS) with state* $\mathbf{x}$*, input* $\mathbf{z}$ *and output* $\mathbf{y}$*:* $\dot{\mathbf{x}} = \mathbf{f}(\mathbf{x}) + \mathbf{g}(\mathbf{x})\mathbf{z}, \mathbf{y} = \mathbf{h}(\mathbf{x})$*, and* ω *a real valued function from* $\mathcal{Z} \times \mathcal{Y} \to \mathbb{R}$*,* $\mathbf{f},\mathbf{g},\mathbf{h}$ *are functions of* $\mathbf{x}$

The system is dissipative with respect to the supply rate ω *if there exists a nonnegative storage function* $V : \mathbb{R}^n \to \mathbb{R}^+$*, such that* $\forall \mathbf{z} \in \mathcal{Z}$*,* $\mathbf{x_0} \in \mathbb{R}^n$*,* $t \geq 0$*,*

$$V(\mathbf{x}(t)) - V(\mathbf{x_0}) \leq \int_0^t \omega(z(\tau), y(\tau))d\tau \tag{6}$$

The system is passive when the supply rate is $\omega = \mathbf{y}^T.\mathbf{z}$ *and* $V(0) = 0$

Definition 3. *(Bao and Lee (2007))* *The system* *(NLS) of Definition 1, where* $x(t) = \Phi(t, t_0, x_0, z)$ *is the state obtained with initial conditions* t_0, x_0 *is locally Zero State Detectable (ZSD) if there exists a neighborhood* $\mathcal{U}$ *of 0 such that* $\forall x \in \mathcal{U}$,
$h(\Phi(t, t_0, x, 0) = 0 \forall t \geq t_0 \geq 0 \implies \lim_{x \to \infty} \Phi(t, t_0, x, 0) = 0$

Proposition 1. *(Bao and Lee (2007))* *The equilibrium* $\mathbf{y} = 0, \mathbf{z} = 0$ *of the passive system (NLS) of Definition 1, for which the storage function* $V(\mathbf{x})$ *is* $\mathcal{C}^1$ *and* $h(\mathbf{x})$ *is* $\mathcal{C}^1$ *is Lyapunov stable if* $V(\mathbf{x})$ *is positive definite or if the system (NLS) is ZSD. In addition, if* $V(\mathbf{x})$ *is radially unbounded, then the equilibrium is globally stable.*

In addition, a nice property of passive system is stabilization by output feedback:

Proposition 2. *(Byrnes et al. (1991))* *Consider the passive system (NLS) of Definition 1, and assume that* $V(\mathbf{x})$ *is positive definite and proper, and the system is ZSD. Consider a function* $\psi : \mathcal{Y} \to \mathcal{U}$ *and* $\mathbf{y}^T \psi(\mathbf{y}) > 0$ *if* $\mathbf{y} \neq 0$, *then the control* $\mathbf{z} = -\psi(\mathbf{y})$ *globally asymptotically stabilizes the equilibrium* $\mathbf{x} = 0$

Port-Hamiltonian systems are closely related and enjoy most the aforementioned properties when the following conditions are met:

Proposition 3. *(Ortega et al. (2002); Crasta et al. (2015))* *A Port-Hamiltonian system for which the Hamiltonian* $\mathcal{H}(\mathbf{x})$ *is bounded from below and the dissipation matrix* $\mathbf{R}(\mathbf{x})$ *is positive definite is passive and* *the Hamiltonian is the storage function.*

As can be seen from propositions (1,2), dissipativity is a desirable property for a Input-Output system, and hence the assistance should transform the PH system of Figure 1 into a dissipative two-port system (e.g. pilot/swashplate). This two-port system will have a new energy $\mathcal{H}_d$, and new interconnection and dissipation matrices $\mathbf{J_d}$ and $\mathbf{R_d}$, which are assigned by the designer to meet

specifications. The control assistance will provide extra power, the idea being to put the closed-loop system under a Port-Hamiltonian form considering scaled inputs, which will generate a new input-output dynamics between the inputs u, e and the outputs f, v of the system, i.e. between the operator and load ports (equation (2) in the linear case). Proposition 4 gives a condition for an assisted system to be Port-Hamiltonian with respect to scaled user (u, f) and environment (v, e) ports, where α, β are scaling factors.

Proposition 4. *Consider the Port-Hamiltonian system described in equation (5). Let* $\mathbf{J_d}, \mathbf{R_d}, \mathcal{H}_d \geq 0$ *be respectively the desired interconnection, damping matrices and energy function,* α *and* β *scaling factors, and* $\mathcal{H}_a = \mathcal{H}_d - \mathcal{H}$ *the assisting energy. If:*

- $\mathbf{R_d}$ *is symmetric and positive definite, and :*
-

$$\mathbf{g}^T \frac{\partial \mathcal{H}_a}{\partial \mathbf{x}} = \mathbf{h}^T \frac{\partial \mathcal{H}_a}{\partial \mathbf{x}} = 0 \tag{7}$$

then the following control assistance $\mathbf{L.a}$*:*

$$\mathbf{L.a} = (\beta - 1)\mathbf{g}.u + (\alpha - 1)\mathbf{h}.e + (\mathbf{J_d}(\mathbf{x}) - \mathbf{R_d}(\mathbf{x}))\frac{\partial \mathcal{H}_d}{\partial \mathbf{x}} - (\mathbf{J}(\mathbf{x}) - \mathbf{R}(\mathbf{x}))\frac{\partial \mathcal{H}}{\partial \mathbf{x}} \tag{8}$$

yields the closed loop system of equation (9), which is dissipative with respect to ports u, f *and* e, v *with supply rates* $\beta f.u$ *and* $\alpha v^T e$*.*

$$\begin{cases} \dot{\mathbf{x}} = (\mathbf{J_d}(\mathbf{x}) - \mathbf{R_d}(\mathbf{x}))\frac{\partial \mathcal{H}_d}{\partial \mathbf{x}} + \beta \mathbf{g}.u + \alpha \mathbf{h}.e \\ f = \mathbf{g}^T \frac{\partial \mathcal{H}}{\partial \mathbf{x}}, v = \mathbf{h}^T \frac{\partial \mathcal{H}}{\partial \mathbf{x}} \end{cases} \tag{9}$$

Proof: if $\mathbf{g}^T \frac{\partial \mathcal{H}_a}{\partial \mathbf{x}} = 0$, then $f = \mathbf{g}^T \frac{\partial \mathcal{H}}{\partial \mathbf{x}} = \mathbf{g}^T \frac{\partial \mathcal{H}_d}{\partial \mathbf{x}}$; in this case, if $e = 0$, one has $\frac{d\mathcal{H}_d}{d\mathbf{t}} = \frac{\partial \mathcal{H}_d^T}{\partial \mathbf{x}} \dot{\mathbf{x}} = \frac{\partial \mathcal{H}_d^T}{\partial \mathbf{x}} \mathbf{R_d}(\mathbf{x}) \frac{\partial \mathcal{H}_d}{\partial \mathbf{x}} + \frac{\partial \mathcal{H}_d^T}{\partial \mathbf{x}} \beta \mathbf{g}.u \leq f \beta u$
The same can be found for the port e, v. This means that the system can be considered, with the help of an assistance, as passive with respect to the inputs with scaled outputs βf and αv. When $\beta = 1, \alpha \neq 1$, one can talk of force-scaling, which is the specific application case considered in this paper. β is the velocity scaling factor, that is, the steady state (static) value of the load velocity, here

the swashplate's, would be β times the open-loop steady value, for the same operator (here pilot stick) velocity. Usually, Port-Hamiltonian systems require that the so-called "matching equation", which in this case is equation (8), be fulfilled. This can always be the case by enforcing an appropriate assistance $\mathbf{L}.\mathbf{a}$. from a formal point of view, it is not necessary to distinguish $\mathbf{L}$ and $\mathbf{a}$, but, however, for simulations and implementation purposes it is necessary to know where to actuate (structurally represented by $\mathbf{L}$) according to a control law (given by $\mathbf{a}$).

$\mathcal{H}_a = \mathcal{H}_d - \mathcal{H}$ is the extra total energy brought to the scaled system, which will bring modifications to the storage units. Condition (7) stipulates that among the storage units (I- and C-elements in Bond-Graphs), those which are linked directly with the user or load ports should not be modified by the assistance. This work can be related to Bond-Graph aided control design, based on structural controllability analysis, allowing input-output decoupling and disturbance rejection (Dauphin-Tanguy et al. (1999)). However, the sufficient conditions given for operator assisting systems are straightforward and do not require any further model/controller checking.

3. AN ENERGETIC REPRESENTATION OF FLIGHT AXIS CONTROL

3.1. Flight axis control overview

Control of the helicopter in flight involves changing the magnitude of rotor thrust or its orientation. The magnitude and direction of the lift which is generated by the rotation of the blades around the rotor mast can be modified by adjusting the angle of incidence of each blade. Moving the cyclic stick allows the pilot to alter the pitch angle of the blades individually as they revolve. On the selected side of the helicopter, the angle of attack (and therefore the lift) is greater thus tilting the rotor and moving the aircraft in the desired direction.

The device in a helicopter control system which feeds the cyclic control movements to the rotor hub is called the swashplate, which consists of an upper and a

lower plate connected with a bearing. The upper plate is linked by pitch control rods to the feathering hinge mechanisms of the blades and rotates with the hub. A CVT including hydraulic actuators, pushrods and bell cranks tilts the non-rotating lower swashplate in any direction in response to the helicopter flight controls (see Raletz (2010); Torenbeek and Wittenberg (2009)). The collective lever is able to raise or lower the swashplate hence changing the angle of attack of the blades simultaneously, and, acting on the rotor lift, allows the helicopter to control its acceleration, hence gain or lose altitude and/or speed. The three main servo-actuators of heavy helicopters can experience 1.5 kN efforts mainly owing to the blade incidence stiffness (see Figures 2 and 3).

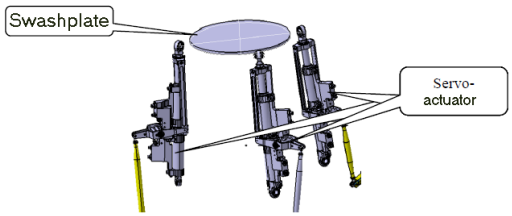

Figure 2: Multibody model of servo-actuators and lower swashplate

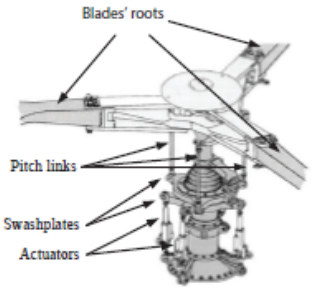

Figure 3: Real swashplate and rotor blade configuration

Tail rotor control aims are to counter the main rotor torque and to maneuver the helicopter around its yaw axis. It has equivalent CVT technological structure to main rotor collective CVT.

Hence, the pilot has to handle two sticks and act on pedals to maneuver the aircraft. A Continuous Variable Transmission links the control handles to the three servo-actuators (main rotor). A number of assisting devices (hydraulic servo controls, dampers, trim, hydraulic jacks) will answer local problems such as vibration damping, or global problems such as aircraft stabilization, pilot

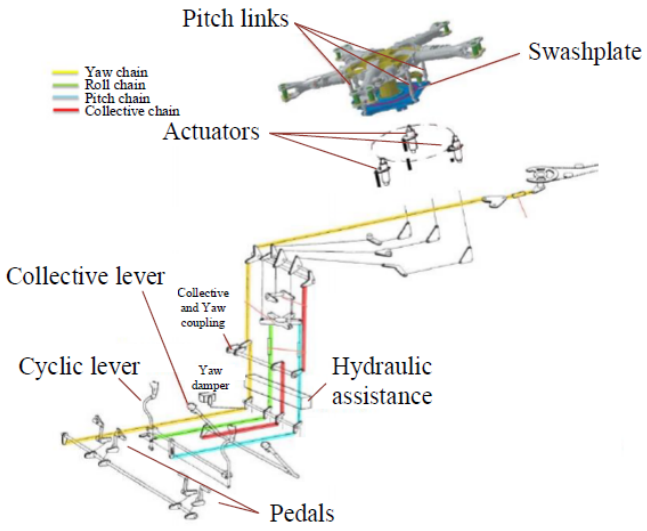

Figure 4: Synoptic of helicopter flight controls

force scaling, lift effort feedback to the pilot.

The scope of this part is to analyze only the force scaling and effort feedback specifications in energetic terms without considering ancillary devices. A simplified model of the four Continuous Variable Transmissions is proposed where control axes couplings are linking the CVT downstream to the control handles and upstream to the swashplate. The biodynamical behavior of the pilot is not considered and can be found in (Tod et al. (2017)).

Depending on the complexity of the helicopter, the cyclic and collective CVTs may be linked together by a mixing unit, a mechanical or hydraulic device that combines the inputs from both CVTs and then sends along the "mixed" input to the swashplate to achieve the desired result. The word Bond-Graph of the structure is represented in Figure 5. Such a model could be derived for example from the works of (Chikhaoui et al. (2012)). In the following sections, only the pitch motion will be considered.

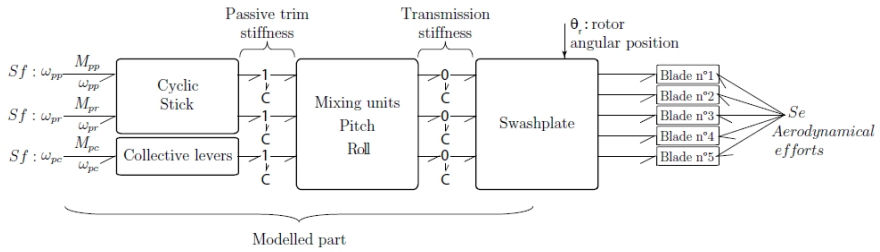

Figure 5: Word Bond Graph of the non assisted CVT

3.2. Equivalent compliance and inertia calculations

In this subsection, it will be shown that the equivalent load of a simplified model of five-blade rotor, referred to the pitch motion of the swashplate, has constant compliance and moment of inertia whatever the rotor position (see Figure 3 to see a 3 blade rotor). The pitch angle θ_{pi} of each blade i depends on the rotor angle θ_r and on the swashplate pitch angle θ_s and their derivatives (see Figure 6). Actuator and pitch links are not modelled, and the blade moment of inertia does not include the hinges; more sophisticated models can be found for example in (Jefferson Allred et al. (2015)) which will however exhibit complicated equations, whereas finding constant inertia and compliance may allow to tune the assistance force scaling factor . The blade pitch control rod generates a rotation of the blade around the longitudinal axis. Under small angle (θ_s, θ_{pi}) approximation, the blade pitch control rod has only a vertical displacement λ_i, the swashplate and rotor are stiff and their masses are negligible, the mechanical work generated by efforts is considered as negligible, the blade pitch angle θ_{pi} is:

$$\theta_{pi} = \frac{\lambda_i}{r_l}, \tag{10}$$

where r_l is the rod length, R the swashplate radius, and for a 5 blades rotor:

$$\lambda_i = R \cdot \sin\left(\theta_r + \frac{2(i-1)\pi}{5}\right) . \tan\left(\theta_s\right) \approx R \cdot \theta_s \sin\left(\theta_r + \frac{2(i-1)\pi}{5}\right) .$$

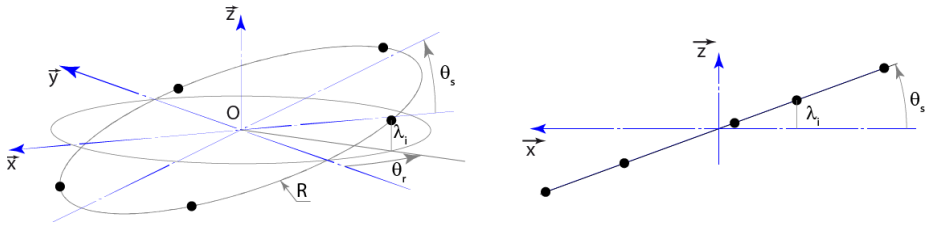

Figure 6: Simplified view of swashplate and blade configurations

Let H_{ps} the total potential energy in the five blade pitch change hinges:

$$H_{ps} = \frac{1}{2}\sum_{i=1}^{5}\frac{1}{C_b}\theta_{pi}^2 = \frac{1}{2}\sum_{i=1}^{5}\frac{1}{C_b}\left(\frac{R}{r_l}\theta_s \sin\left(\theta_r + \frac{2(i-1)\pi}{5}\right)\right)^2,$$

C_b is the blade-rod joint compliance of one blade. Remarking that $\sum_{i=1}^{5}\sin^2\left(\theta_r + \frac{2(i-1)\pi}{5}\right) = \frac{5}{2}$, one obtains

$H_{ps} = \frac{1}{2}\frac{1}{C_b}\frac{5}{2}\frac{R^2}{r_l^2}\theta_s^2$. The equivalent compliance referred to the load C_s is :

$$C_s = \frac{2r_l^2 C_b}{5R^2}. \tag{11}$$

The same applies for the calculation of the equivalent kinetic energy H_{ks} related to the load.

$$H_{ks} = \frac{1}{2}\sum_{i=1}^{5} I_b \dot{\theta}_{pi}^2$$

where I_b is the moment of inertia of one blade around its pitch axis where

$$\dot{\theta}_{pi} = \dot{\theta}_s \frac{R}{r_l}\sin\left(\theta_r + \frac{2(i-1)\pi}{5}\right) + \theta_s \frac{R}{r_l}\dot{\theta}_r \cos\left(\theta_r + \frac{2(i-1)\pi}{5}\right).$$

As the pitch motion is independent from $\dot{\theta}_r$ (that does not depend on $\dot{\theta}_s$), and as the sum of the cross-products is equal to zero:

$$\sum_{i=1}^{5}\sin\left(\theta_r + \frac{2(i-1)\pi}{5}\right)\cos\left(\theta_r + \frac{2(i-1)\pi}{5}\right) = \frac{1}{2}\sum_{i=1}^{5}\sin\left(2\theta_r + \frac{4(i-1)\pi}{5}\right) = 0,$$

the expression of the equivalent kinetic energy H_{ks} reduces to

$$H_{ks} = \frac{5}{2}\frac{R^2}{r_l^2} I_b \dot{\theta}_s^2,$$

and the equivalent inertia is

$$I_s = \frac{5\, R^2}{r_l^2} I_b. \tag{12}$$

which will justify that the equivalent load has kinetic and potential energies that are considered, in the sequel, as independent from the rotor position θ_r.

3.3. Bond-Graph and Port Hamiltonian representation of helicopter flight axis

It is recalled from figure 5 that the stick velocity ω_p is transmitted through a Continuous Variable Transmission to the swashplate, with equivalent inertia I_s and compliance C_s calculated in equation (11-12). The simplified Bond-Graph model proposed in Figure 7 includes the compliances of the stick and lower linkage C_{ll}, of the trim C_{pt} , and of upper linkage C_{ul}, I_l is the moment of inertia of the CVT linkage. The transformer (TF) element with gain k accounts for the global kinematic gain of the CVT. Resistive elements are not shown for the sake of readability. All specific notations are given in section 6.

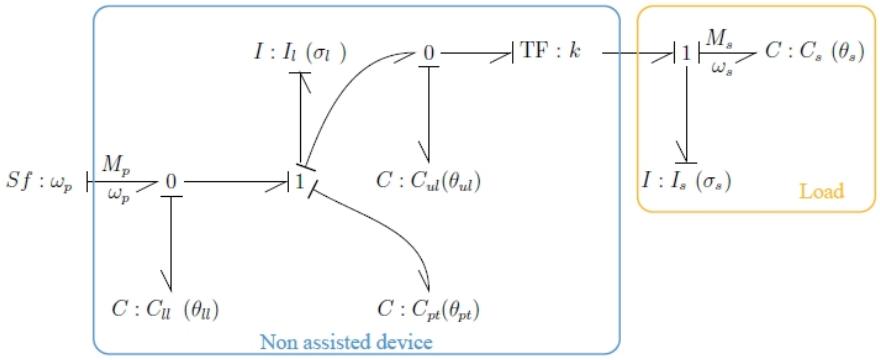

Figure 7: Bond-Graph of the non assisted CVT

The Port-Hamiltonian model follows immediately with the total energy $\mathcal{H} = \frac{1}{2}\mathbf{x}^T\mathbf{S}\mathbf{x}$, where $\mathbf{x}$ is the state-space vector, $\mathbf{x} = \begin{pmatrix} \theta_{ll} & \sigma_l & \theta_{pt} & \theta_{ul} & \sigma_s & \theta_s \end{pmatrix}^T$ The input ports for the operator, load and assistance ports are respectively the pilot stick speed ω_p, the swashplate load torque M_s and the assisting vector

(force) **L.a**, which is to be determined. The collocated outputs are the pilot torque feedback M_p, the swashplate speed ω_s and a reaction velocity **b** exerted at the assistance port. Equation (5) turns to :

$$\begin{cases} \dot{\mathbf{x}} = (\mathbf{J}(\mathbf{x}) - \mathbf{R}(\mathbf{x}))\frac{\partial \mathcal{H}}{\partial \mathbf{x}} + \mathbf{g}.\omega_p + \mathbf{h}.M_s + \mathbf{L}.\mathbf{a} \\ M_p = \mathbf{g}^T \frac{\partial \mathcal{H}}{\partial \mathbf{x}}, \omega_s = \mathbf{h}^T \frac{\partial \mathcal{H}}{\partial \mathbf{x}}, b = \mathbf{L}^T \frac{\partial \mathcal{H}}{\partial \mathbf{x}} \end{cases} \tag{13}$$

with matrices $\mathbf{g}, \mathbf{h}, \mathbf{S}, \mathbf{J}, \mathbf{R}$

$$\mathbf{g} = \begin{pmatrix} 1 & 0 & 0 & 0 & 0 & 0 \end{pmatrix}^T, \mathbf{h} = \begin{pmatrix} 0 & 0 & 0 & 0 & 1 & 0 \end{pmatrix}^T$$

$$\mathbf{J} = \begin{bmatrix} 0 & -1 & 0 & 0 & 0 & 0 \\ 1 & 0 & -1 & -1 & 0 & 0 \\ 0 & 1 & 0 & 0 & 0 & 0 \\ 0 & 1 & 0 & 0 & -k & 0 \\ 0 & 0 & 0 & k & 0 & -1 \\ 0 & 0 & 0 & 0 & 1 & 0 \end{bmatrix}$$

$$\mathbf{R} = \begin{bmatrix} 0 & 0 & 0 & 0 & 0 & 0 \\ 0 & R_{ul} + R_l & 0 & 0 & -R_{ul} \cdot k & 0 \\ 0 & 0 & 0 & 0 & 0 & 0 \\ 0 & 0 & 0 & 0 & 0 & 0 \\ 0 & -R_{ul} \cdot k & 0 & 0 & R_{ul} \cdot k^2 + R_s & 0 \\ 0 & 0 & 0 & 0 & 0 & 0 \end{bmatrix}$$

$$\mathbf{S} = \begin{bmatrix} \frac{1}{C_{ll}} & 0 & 0 & 0 & 0 & 0 \\ 0 & \frac{1}{I_l} & 0 & 0 & 0 & 0 \\ 0 & 0 & \frac{1}{C_{pt}} & 0 & 0 & 0 \\ 0 & 0 & 0 & \frac{1}{C_{ul}} & 0 & 0 \\ 0 & 0 & 0 & 0 & \frac{1}{I_s} & 0 \\ 0 & 0 & 0 & 0 & 0 & \frac{1}{C_s} \end{bmatrix}$$

We can notice that $\mathbf{R} \succ 0, \mathbf{S} \succ 0$, and $\mathbf{J}$ is skew-symmetric.

3.4. Control specifications and design

Piloting a helicopter needs expert skills, the mechanical and aerodynamical behavior of the aircraft being complex with at least four controls (including the collective lever, cyclic stick, and anti-torque pedal) to activate. Current high-weight helicopters need an assistance to alleviate the pilot muscular strain, i.e. this assistance should perform force scaling. Load feedback should be felt stiffer when the aircraft experiences a turn or a change in heading, and smoother in regular flight conditions. A smooth $\mathcal{C}^1$ characteristics has been chosen to approximate a piecewise linear map to avoid singularities. The stick force vs. position specifications which are given Figure 8 meet these requirements, with appropriate values. On the figure, this map is compared with classical existing linear trim.

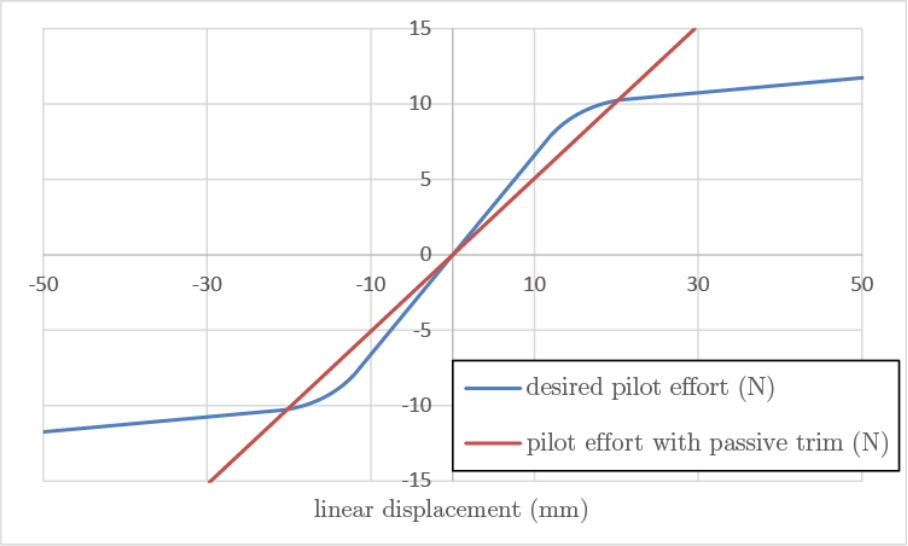

Figure 8: Stick effort-position specifications

The energy of the CVT is reshaped by introducing a PTF element before the swashplate with scaling factor $\frac{k}{\alpha}$ as shown in the Bond-Graph of the closed-loop system (Figure 9). Besides, the overall dynamical structure is kept (see Figures

7 and 9) , but the passive trim is turned into an “active trim” with the new non constant trim compliance C_{at} justified by the specifications and shown in Figure 8. It means that not only Energy Shaping techniques are used, but the internal dynamics (interconnextion and damping matrices) is modified which is related to the Interconnection and Damping Assignment Passivity-Based Control (IDA-PBC) technique (Ortega et al. (2002)). Note that the new behavior is not passive as the MSe elements imply that external power is injected through the assistance $L.a$ described in equation (20).

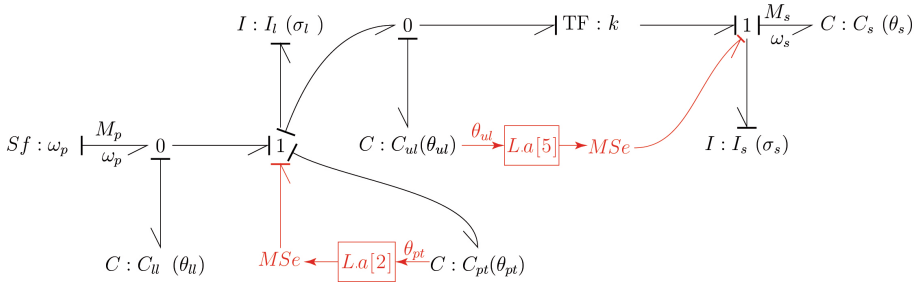

Figure 9: Bond Graph of the specified closed-loop assisted system

The application of the dissipative control design equations (8-9), with the kinematic scaling factor $\beta = 1$, yields the assistance :

$$\mathbf{L.a} = (\alpha - 1)\mathbf{h}.M_s + (\mathbf{J_d}(\mathbf{x}) - \mathbf{R_d}(\mathbf{x}))\frac{\partial \mathcal{H}_d}{\partial \mathbf{x}} - (\mathbf{J}(\mathbf{x}) - \mathbf{R}(\mathbf{x}))\frac{\partial \mathcal{H}}{\partial \mathbf{x}}, \tag{14}$$

and the closed-loop dynamical behavior :

$$\begin{cases} \dot{\mathbf{x}} = (\mathbf{J_d}(\mathbf{x}) - \mathbf{R_d}(\mathbf{x}))\frac{\partial \mathcal{H}_d}{\partial \mathbf{x}} + \mathbf{g}.\omega_p + \alpha \mathbf{h}.M_s \\ M_p = \mathbf{g}^T \frac{\partial \mathcal{H}}{\partial \mathbf{x}}, \omega_s = \mathbf{h}^T \frac{\partial \mathcal{H}}{\partial \mathbf{x}}. \end{cases} \tag{15}$$

with matrices $\mathbf{S_d}, \mathbf{J_d}, \mathbf{R_d}$, with $\mathbf{R_d} \succ 0, \mathbf{S_d} \succ 0$:

$$\mathbf{J_d} = \begin{bmatrix} 0 & -1 & 0 & 0 & 0 & 0 \\ 1 & 0 & -1 & -1 & 0 & 0 \\ 0 & 1 & 0 & 0 & 0 & 0 \\ 0 & 1 & 0 & 0 & -(\alpha+1)k/2 & 0 \\ 0 & 0 & 0 & (\alpha+1)k/2 & 0 & -1 \\ 0 & 0 & 0 & 0 & 1 & 0 \end{bmatrix}$$

$$\mathbf{R_d} = \begin{bmatrix} 0 & 0 & 0 & 0 & 0 & 0 \\ 0 & R_{ul}+R_l & 0 & 0 & -R_{ul}\cdot k & 0 \\ 0 & 0 & 0 & 0 & 0 & 0 \\ 0 & 0 & 0 & 0 & (\alpha-1)k/2 & 0 \\ 0 & -R_{ul}\cdot k & 0 & (\alpha-1)k/2 & R_{ul}\cdot k^2+R_s & 0 \\ 0 & 0 & 0 & 0 & 0 & 0 \end{bmatrix}$$

$$\mathbf{S_d} = \begin{bmatrix} \frac{1}{C_{ll}} & 0 & 0 & 0 & 0 & 0 \\ 0 & \frac{1}{I_l} & 0 & 0 & 0 & 0 \\ 0 & 0 & \frac{1}{C_{at}} & 0 & 0 & 0 \\ 0 & 0 & 0 & \frac{1}{C_{ul}} & 0 & 0 \\ 0 & 0 & 0 & 0 & \frac{1}{I_s} & 0 \\ 0 & 0 & 0 & 0 & 0 & \frac{1}{C_s} \end{bmatrix}$$

and, eventually, the control law stemming from equation (14)is:

$$L\cdot a = \begin{Bmatrix} 0 \\ \theta_{pt}\left(\frac{1}{C_{pt}}-\frac{1}{C_{at}}\right) \\ 0 \\ 0 \\ \left(-\frac{R_{ul}}{I_l}\sigma_l-\frac{k}{C_{ul}}\theta_{ul}+\frac{R_{ul}k^2}{I_s}\sigma_s\right)(1-\alpha) \\ 0 \end{Bmatrix}$$

Note that the state space $\mathbf{x}$ remains the same as before, as the structure was not modified by the assistance. Of course, the implementation of the assistance

requires that the torque M_s and the state space vector $\mathbf{x}$ be measured. When the measures are not available, it is possible to use state or load observers, which is beyond the scope of this paper.

4. SIMULATIONS

4.1. Software architecture and validation procedure

As seen in the previous section, control laws have been designed using the simplified Bond-Graph and Port-Hamiltonian models of Figures 7 and 9. Simulations have been performed using the 20-sim®, dedicated to simulate multi-domain lumped parameters models using Bond Graphs.

It was sought to apply these control laws on a more realistic system. A multi-body model of the helicopter flight controls Continuous Variable Transmission, has been designed under LMS Virtual.Lab ® suite, including actuators and sensors. One can see from Figure 10 that the control laws designed and validated in a first time with 20-sim are represented as block diagrams in the LMS Imagine.Lab ® software. Next, control equations are sent after compilation to the mechanical model and considered by the LMS Virtual.Lab ® solver, therefore integrating the global closed-loop dynamics of the flight control system.

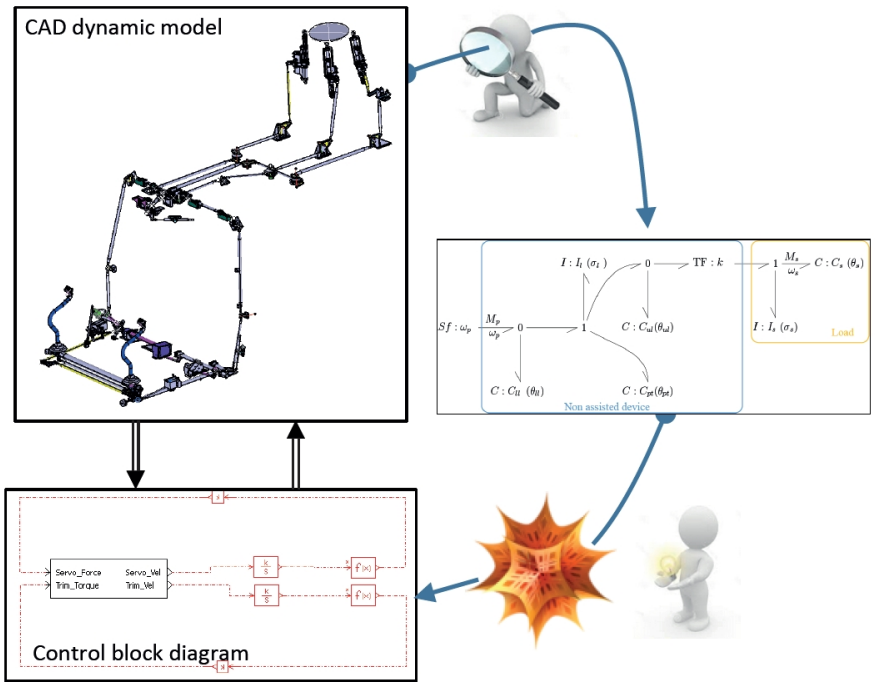

Figure 10: Synoptics of the simulation strategy

Figure 11 shows, as an example, the multibody representation of the cyclic (pitch and roll) control stick and passive trim.

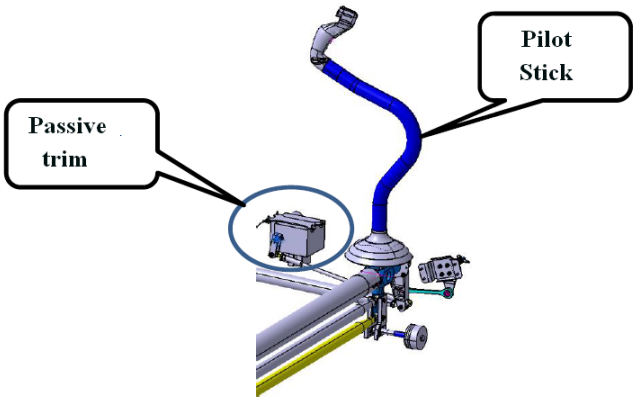

Figure 11: Passive trim and stick modelling

In the simulations section, the 20-sim simulation is compared with the multi-body representation under assistance. Eventually, the stick position/effort diagram is compared with the specifications and a real-life profile.

4.2. Simulation results

Figure 12 shows that the swashplate angle follows nearly perfectly the motion reference delivered by the stick, with a precision less than 0.1° which means that trajectory following is considered as achieved, i.e. with a kinematic scaling factor $\beta = 1$. Eventually, this allows to assess the controller's performance.

- Position-force maps show a hysteretic behavior which are related, in reality, to dissipation due to viscous friction.

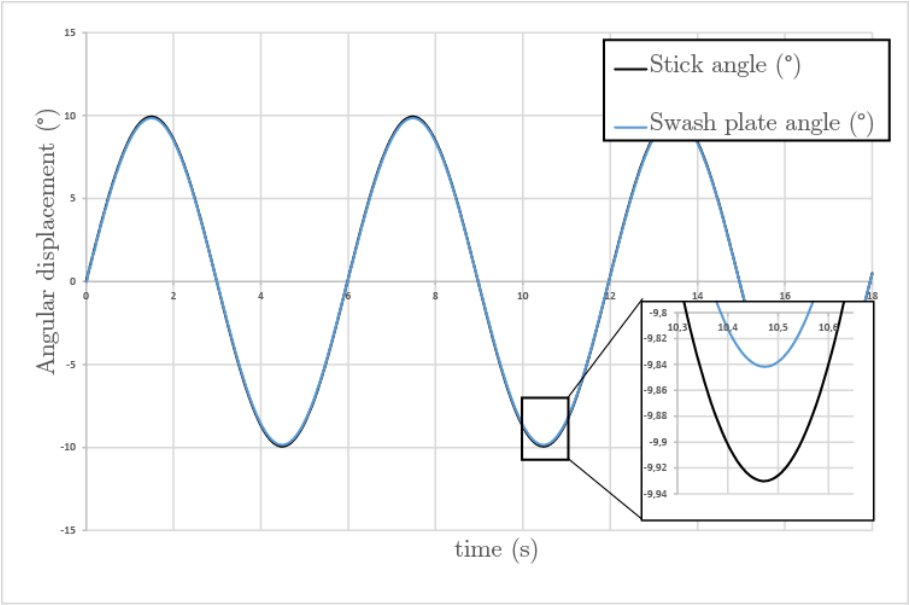

Figure 12: Swashplate and stick (reference) angles

Figure 13 shows the pilot stick force/position map of the system under assistance. The behavior of the closed-loop Bond-Graph model is quite similar to the multibody model under assistance, and follows approximately the specifications. Globally, the force-displacement maps are quite similar when using the port-Hamiltonian simplified model and the multibody model under the designed assistance, and both are themselves quite close to a real helicopter behavior with the current assistance. The deviations are due to model discrepancies (linear vs. nonlinear multibody model). However, the linearized PH model, which is useful for analysis and control design, becomes less accurate for displacements over 25 mm. The multibody model includes nonlinearities such as a non constant kinematic gain k (which varies in a range of $\pm 15\%$, and considered as constant in the PH simplified model).Of course, it could be possible to refine the PH model, but then more parameters should be accurately known, and the design might be more complicated and may be less robust in case of parameter mismatch.

The desired effort characteristics is specified for static conditions. The simulation of dynamical phenomena (viscous friction) results in an hysteretic behavior. Consequently, for a same position, the effort will be different when considering the forward and reverse paths. Improving the model would require a very good estimate of the viscous friction parameters which is quite uneasy. Also light oscillations can be seen that are related to the slightly low stiffness of the links.

The behavior is not exactly centered on the specified characteristics, because a small part of the pilot effort is dedicated to the start-up of the swashplate (once again, due to local compliance and friction). One possibility would be to include dry friction in the model, which is possible for Port-hamiltonian systems, but once again, model parameters may be hard to identify (Koopman et al. (2011)). A perspective would be to solve the problem at the multibody level with the same theoretical approach. This could be done using coordinate dependent port-Hamiltonian matrices such as in (Donaire and Perez (2012)), at the price of losing the simplicity of the controller's equations. In this specific case, this does not seem to be mandatory as results are already satisfactory.

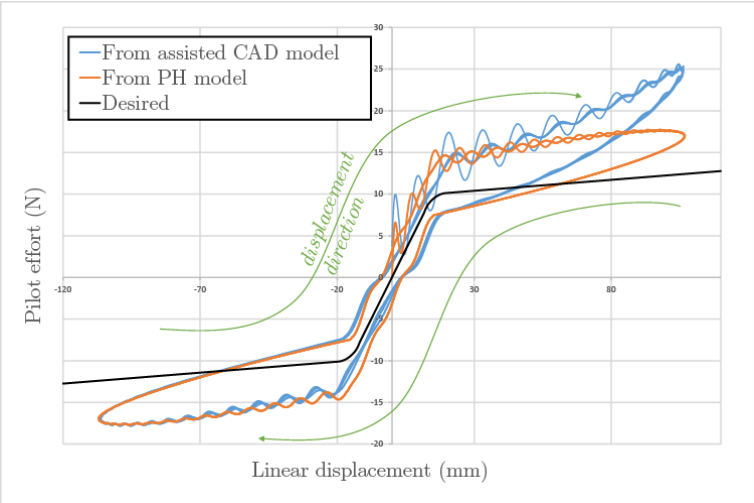

Figure 13: Force feedback-displacement map of the pilot stick for CAD and simplified (PH) models

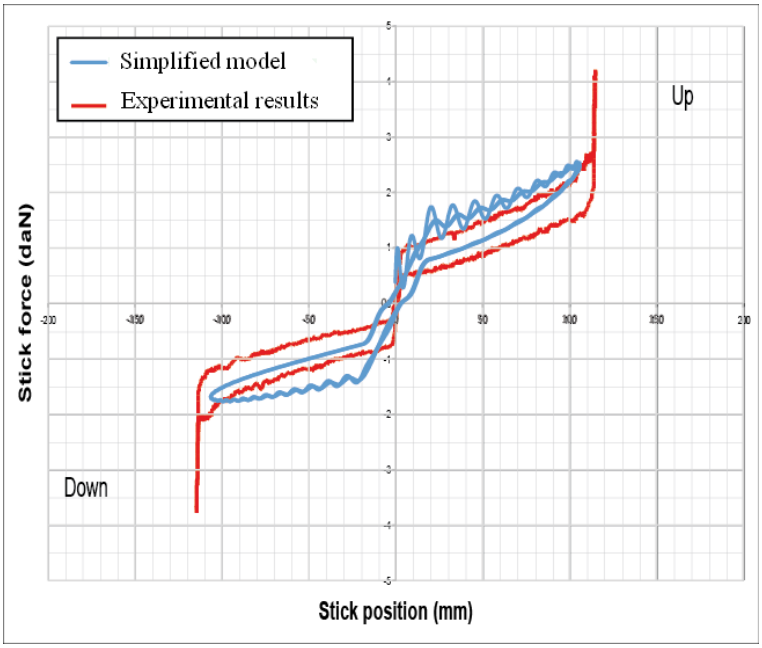

Figure 14: A real pilot stick force/position map

Figure 14 shows a real helicopter stick force/position map, which profile is quite close to that which has been obtained for the CAD model under assistance. As a conclusion, it can be said that the simplified assisting controller design method is relevant. The energetic representation was not intended to solve every problems, but can contribute to a better understanding of power flows in the helicopter; that is, one knows from the assistance design where external power enters the CVT, and from the Bond-Graph, where power is dissipated or stored. This can be of a help to identify, for example, energy circles that can cause instabilities, which is beyond the scope of this paper but is handled in Tod et al. (2017).

5. CONCLUSION

Operator Assisting Systems were represented under the port-Hamiltonian framework, the main challenge being to know where and how the assistance should be applied within the Continuous Variable Transmission. Conditions were proposed under which the closed-loop system under assistance remained dissipative. These conditions were relaxed for linear systems. The results were applied to helicopter pitch control, viewed as an assistance to the pilot. Under this assistance, the control effort was scaled up, the rotor was tilted in the right position and force feedback was sent to the pilot. The results applied to a multibody representation of the flight axis controls were found to be close to that found of a real assisted system. Hence, this simple and generic method, which offers physical and energetic insight, is a good start-point for helicopter flight axis control, and, in general, of Operator Assisting Systems design. In the future, the relevance of partial fly-by-wire controls will be explored. The application of the methodology to other kinds of manipulators, with several load points, such as exoskeletons, will also be investigated.

6. Helicopter CVT Notations

Main Bond-Graph notations Subscripts

M	torque
ω	rotational speed
θ	angle
σ	momentum
I	inertia
C	compliance
R	damping factor
k	kinematic gain
α	torque scale factor

p	pilot
s	swashplate
l	CVT linkage
ll	lower linkage
ul	upper linkage
m	modulated torque
pt	passive trim
at	active trim

Input-output notations

u, f	operator velocity/effort
v, e	load velocity/effort
$\mathbf{a}, b$	assistance effort/reactio velocity
$\mathbf{H}$	H-matrix
$_d$	subscript for desired
γ_F, γ_E	flow and effort scaling factors

Port-Hamiltonian notations

$\mathbf{x}$	state vector
$\mathbf{g}, \mathbf{h}$	input pilot, load vectors
$\mathbf{L}$	input assistance matrix
$\mathbf{R}$	dissipation matrix
$\mathbf{J}$	interconnection matrix
β	velocity scale factor
$\mathcal{H}$	Hamiltonian

Bao, J. and Lee, P. (2007). *Process Control: The Passive Systems Approach*. Springer-Verlag.

Byrnes, C. I., Isidori, A., and Willems, J. C. (1991). Passivity, feedback equivalence, and the global stabilization of minimum phase nonlinear systems. *IEEE Transaction on Automatic Control*, 36:1228–1240.

Chikhaoui, Z., Gomand, J., Malburet, F., and Barre, P. (2012). *Complementary Use of BG and EMR Formalisms for Multiphysics Systems Analysis and Control*, volume 4. ASME. Engineering Systems Design and Analysis.

Crasta, N., Ortega, R., and Pillai, H. K. (2015). On the matching equations of

energy shaping controllers for mechanical systems. *International Journal of Control*, 88:1757–1765.

Dauphin-Tanguy, G., Rahmani, A., and Sueur, C. (1999). Bond graph aided design of controlled systems. *Simulation Practice and Theory*, 7:493–513.

De Santis, A., Siciliano, B., De Luca, A., and Bicchi, A. (2008). An atlas of physical human-robot interaction. *Mechanism and Machine Theory*, 43:253–270.

Donaire, A. and Perez, T. (2012). Dynamic positioning of marine craft using a port-hamiltonian framework. *Automatica*, 48:851–856.

Ferraguti, F., Preda, N., Manurung, A., Bonfe, M., Lambercy, O., Gassert, R., Muradore, R., Fiorini, P., and Secchi, C. (2015). An energy tank-based interactive control architecture for autonomous and teleoperated robotic surgery. *IEEE Transactions on Robotics*, 31:1073–1088.

Friedman, C. and Rand, O. (2015). Robust trim procedure for rotorcraft configurations. *Aerospace Science and Technology*, 45:442–448.

Hannaford, B. (1989). A design framework for teleoperators with kinesthetic feedback. *IEEE Transactions on Robotics and Automation*, 5:426–434.

Hogan, N. (1985). Impedance control: an approach to manipulation. *Journal of Dynamic Systems, Measurement, and Control*, 107:1–24.

Jazayeri, A. and Tavakoli, M. (2016). Bilateral teleoperation system stability with non-passive and strictly passive operator or environment. *Control Engineering Practice*, 40:45–60.

Jefferson Allred, C., Jolly, M. R., and Buckner, G. D. (2015). Real-time estimation of helicopter blade kinematics using integrated linear displacement sensors. *Aerospace Science and Technology*, 42:274–286.

Kazerooni, H. (1990). Human-robot interaction via the transfer of power and information signals. *IEEE Transactions on Systems, Man, and Cybernetics*, 20:450–463.

Koopman, J., Jeltsema, D., and Verhaegen, M. (2011). Port-hamiltonian description and analysis of the lugre friction model. *Simulation Modelling Practice and Theory*, 19:959–968.

Lacevic, B. and Rocco, P. (2011). Closed-form solution to controller design for human-robot interaction. *Journal of Dynamic Systems, Measurement, and Control*, 133:024501–1–024501–7.

Lee, S., Ha, C., and Kim, B. (2005). Adaptive nonlinear control system design for helicopter robust command augmentation. *Aerospace Science and Technology*, 9:241–251.

Li, P. Y. and Ngwompo, R. (2005). Power scaling bond graph approach to the passification of mechatronic systems - with application to electrohydraulic valves. *Journal of Dynamic Systems, Measurement, and Control*, 127:633–641.

McKillip, R. and Perri, T. (1992). Helicopter flight control system design and evaluation using controller inversion techniques. *Journal of American Helicopter Society*, 37:66–74.

Ortega, R., van der Schaft, A., Maschke, B., and Escobar, G. (2002). Interconnection and damping assignment passivity based control of port-controlled hamiltonian systems. *Automatica*, 38:585–596.

Raletz, R. (2010). *Basic theory of the helicopter*. Cepadues Editions.

Richter, H. (2015). A framework for control of robots with energy regeneration. *Journal of Dynamic Systems, Measurement, and Control*, 137:091004–1–091004–11.

Secchi, C., Stramigioli, S., and Fantuzzi, C. (2007). *Control of interactive robotic interfaces: A port-Hamiltonian approach*. Springer-Verlag.

Secchi, C., Stramigioli, S., and Fantuzzi, C. (2015). Transparency in port-hamiltonian-based telemanipulation. *IEEE Transactions on Robotics*, 24:903–910.

Simplício, P., Pavel, M., van Kampen, E., and Chu, Q. (2013). An acceleration measurements-based approach for helicopter nonlinear flight control using incremental nonlinear dynamic inversion. *Control Engineering Practice*, 21:1065–1077.

Tod, G., Pavel, M., Malburet, F., Gomand, J., and Barre, P.-J. (2017). Understanding pilot biodynamical feedthrough coupling in helicopter adverse roll axis instability via lateral cyclic feedback control. *Aerospace Science and Technology*, 59:18–31.

Torenbeek, E. and Wittenberg, H. (2009). *Flight physics, Chap. 8: Helicopter Flight Mechanics, pp.405-430*. Springer.

Wang, H. and Xie, Y. (2012). Task-space framework for bilateral teleoperation with time delays. *Journal of Dynamic Systems, Measurement, and Control*, 134:051010–1–051010–10.

Worsnopp, T., Peshkin, M., Lynch, K., and Colgate, J. E. (2006). Controlling the apparent inertia of passive human-interactive robots. *Journal of Dynamic Systems, Measurement, and Control*, 128:44–52.

Zhu, D., Zhou, D., Zhou, J., and Teo, K. L. (2012). Synchronization control for a class of underactuated mechanical systems via energy shaping. *Journal of Dynamic Systems, Measurement, and Control*, 134:041007–1–041007–11.